

## Supporting Information

### **Boost the Large Driving Photovoltages for Overall Water Splitting in Direct Z-Scheme Heterojunctions by Interfacial Polarizations**

Xu Gao<sup>1,‡</sup>, Yanqing Shen<sup>1,‡,\*</sup>, Jiajia Liu<sup>1</sup>, Lingling Lv<sup>1</sup>, Min Zhou<sup>1</sup>, Zhongxiang Zhou<sup>1</sup>, Yuan Ping Feng<sup>2</sup>, Lei Shen<sup>3,\*</sup>

<sup>1</sup> *School of Physics, Harbin Institute of Technology, Harbin 150001, PR China*

<sup>2</sup> *Department of Physics, National University of Singapore, Singapore 117551*

<sup>3</sup> *Department of Mechanical Engineering, National University of Singapore, Singapore 117575*

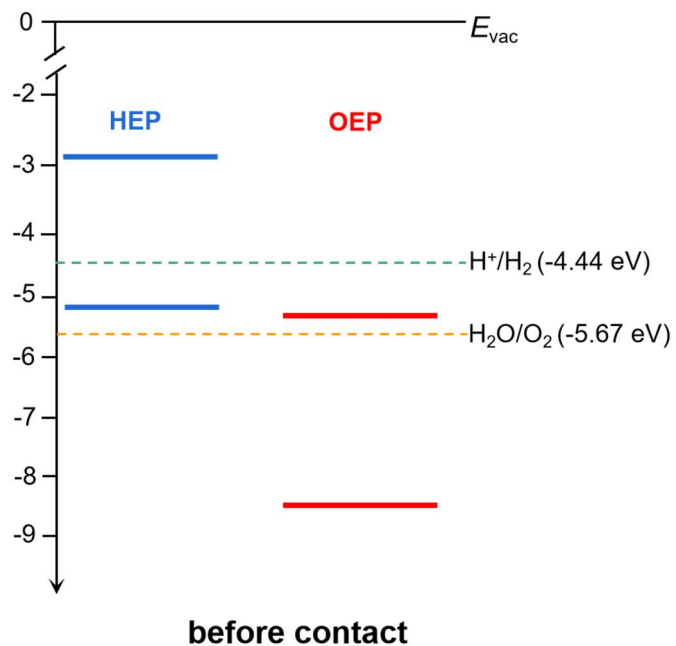


**Fig. S1** Schematic of band alignments with respect to the vacuum level of the two materials (a HEP and an OEP) composing the direct Z-scheme heterojunction before contact. The green and orange dashed lines represent the reduction potential and oxidation potential of water splitting, respectively.

**Table S1** Calculated lattice constants ( $a = b$ ), equilibrium interlayer distance ( $d$ ), interfacial thickness ( $h$ ), interfacial binding energy ( $E_b$ ), dipole moment ( $\mu$ ), electrostatic potential difference ( $\Delta\Phi$ ) and the magnitude of internal electric field ( $E_{\text{int}}$ ) of the PtO<sub>2</sub>-based heterojunction, as well as those of the isolated monolayers after full geometric optimization.

Material	$a = b$ (Å)	$d$ (Å)	$h$ (Å)	$E_b$ (eV)	$\mu$ (Debye)	$\Delta\Phi$ (eV)	$E_{\text{int}}$ (V/Å)
PtO <sub>2</sub> /MoSe <sub>2</sub>	3.24	2.77	5.35	-0.24	0.14	0.55	0.10
PtO <sub>2</sub> /WSe <sub>2</sub>	3.24	2.66	5.37	-0.31	0.18	0.70	0.13
PtO <sub>2</sub> /GeC	3.22	2.87	3.56	-0.26	0.25	0.98	0.27
PtO <sub>2</sub>	3.15	-	-	-	0	0	0
MoSe <sub>2</sub>	3.32	-	-	-	0	0	0
WSe <sub>2</sub>	3.33	-	-	-	0	0	0
GeC	3.25	-	-	-	0	0	0

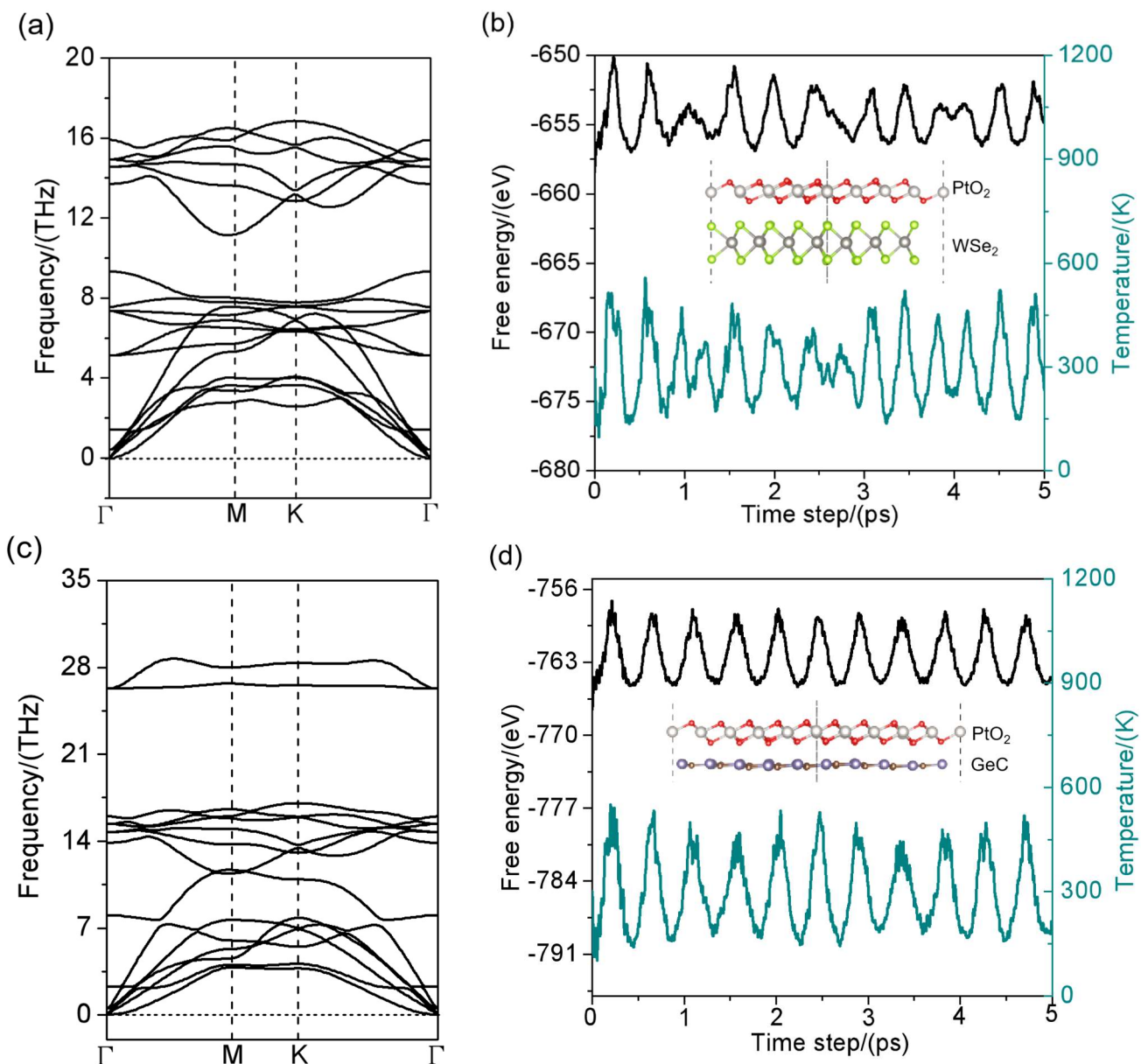


**Fig. S2** Phonon dispersion and molecular dynamics simulations at 300 K of the heterojunction (a-b) PtO<sub>2</sub>/WSe<sub>2</sub>, and (c-d) PtO<sub>2</sub>/GeC. The final configurations are shown as the insets.  $4 \times 4 \times 1$  supercell (96 atoms in total) and  $5 \times 5 \times 1$  supercell (125 atoms in total) are adopted, respectively.

The phonon dispersion and molecular dynamics simulations of PtO<sub>2</sub>/WSe<sub>2</sub>, and PtO<sub>2</sub>/GeC show that there are no imaginary modes in the Brillouin zone (Figs. S2(a) and S2(c)), and there are no obvious structural deformations or broken bonds after 5 ps (Figs. S2(b) and S2(d)). These together imply the robust dynamical and thermal stabilities of the heterojunction PtO<sub>2</sub>/WSe<sub>2</sub> and PtO<sub>2</sub>/GeC.

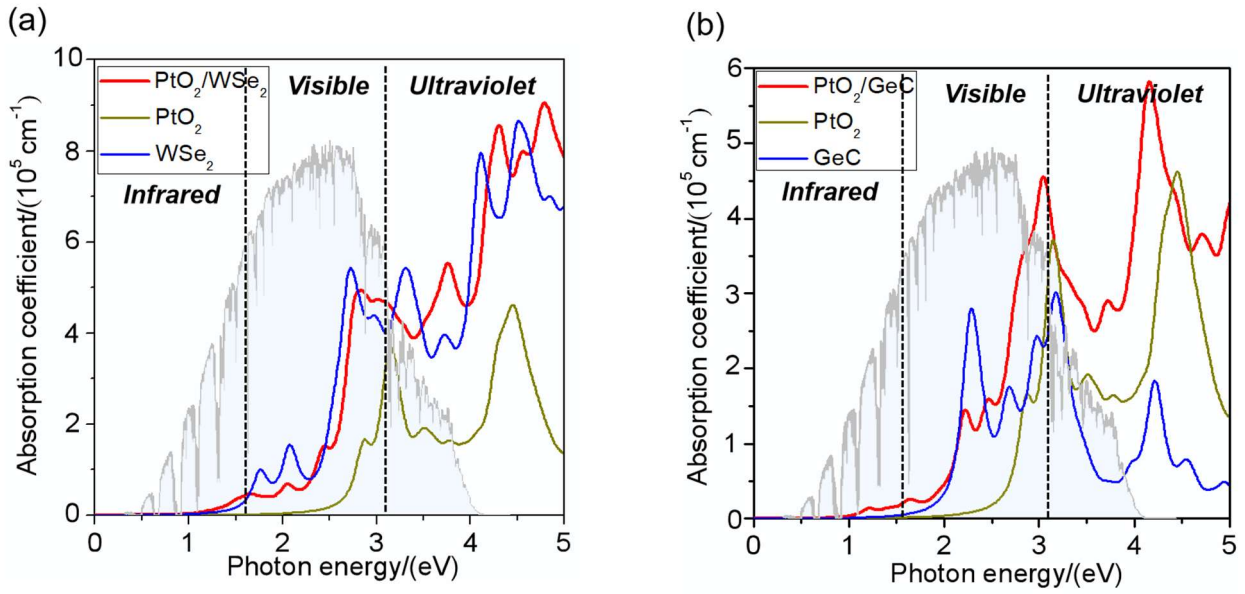


**Fig. S3** Optical absorption spectrum of the heterojunction (a) PtO<sub>2</sub>/WSe<sub>2</sub>, and (b) PtO<sub>2</sub>/GeC, as well as the isolated monolayers PtO<sub>2</sub> and MoSe<sub>2</sub> (GeC) for comparison calculated by  $G_0W_0 + \text{BSE}$  approach.

It can be observed that the heterojunction PtO<sub>2</sub>/WSe<sub>2</sub> (GeC) exhibits significant absorbance of the solar spectrum inclusive of NIR light. Besides, the absorption spectrum exhibits a “red shift” as compared to its parents of monolayers with high absorption coefficient of  $10^5 \text{ cm}^{-1}$ .

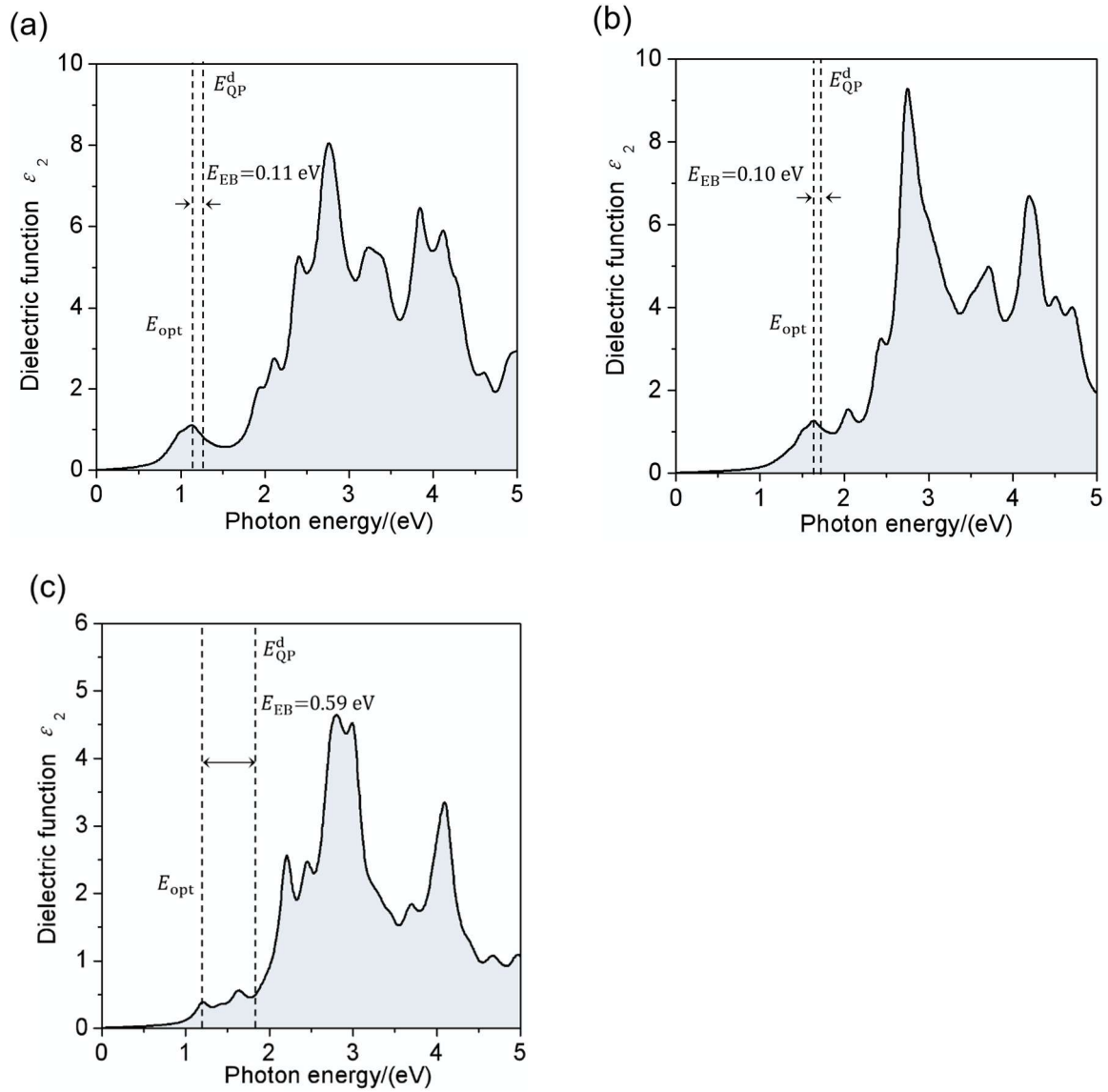


**Fig. S4** Dielectric imaginary part of the heterojunction (a) PtO<sub>2</sub>/MoSe<sub>2</sub>, (b) PtO<sub>2</sub>/WSe<sub>2</sub> and (c) PtO<sub>2</sub>/GeC using  $G_0W_0 + BSE$  approach.  $E_{QP}^d$  and  $E_{opt}$  are the minimum direct quasiparticle band gap and optical band gap, respectively.  $E_{EB}$  is the exciton binding energy.

**Table S2** Corresponding electronic properties of the studied PtO<sub>2</sub>-based heterojunction, including the band gap at HSE06 level ( $E_{\text{HSE06}}$ ), quasiparticle band gap ( $E_{\text{QP}}^i$ ) given by G<sub>0</sub>W<sub>0</sub> approach, minimum direct quasiparticle band gap ( $E_{\text{QP}}^d$ ), optical band gap ( $E_{\text{opt}}$ ) given by G<sub>0</sub>W<sub>0</sub> + BSE approach, exciton binding energy ( $E_{\text{EB}}$ ), and the external potentials provided by photogenerated electrons ( $U_e$ ) and holes ( $U_h$ ) when under light.

Material	$E_{\text{HSE06}}$ (eV)	$E_{\text{QP}}^i$ (eV)	$E_{\text{QP}}^d$ (eV)	$E_{\text{opt}}$ (eV)	$E_{\text{EB}}$ (eV)	$U_e$ (V)	$U_h$ (V)
PtO <sub>2</sub> /MoSe <sub>2</sub>	0.29	0.82	1.24	1.13	0.11	1.48	3.94
PtO <sub>2</sub> /WSe <sub>2</sub>	0.46	1.21	1.70	1.60	0.10	1.44	3.91
PtO <sub>2</sub> /GeC	0.63	1.43	1.80	1.21	0.59	2.18	3.99
PtO <sub>2</sub>	3.25	3.52	4.20	2.86	1.34	-	3.44
MoSe <sub>2</sub>	1.82	2.06	2.06	1.63	0.43	0.74	-
WSe <sub>2</sub>	1.93	2.21	2.21	1.75	0.46	1.09	-
GeC	2.79	3.17	3.17	2.25	0.92	2.03	-

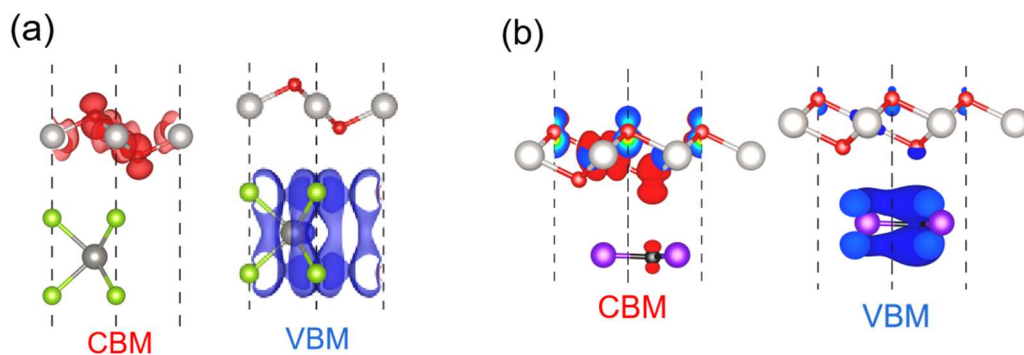


**Fig. S5** Partial charge densities of CBM/VBM of the heterojunction (a) PtO<sub>2</sub>/WSe<sub>2</sub> and (b) PtO<sub>2</sub>/GeC, and the isosurface value is 0.005 e/Å<sup>3</sup>.

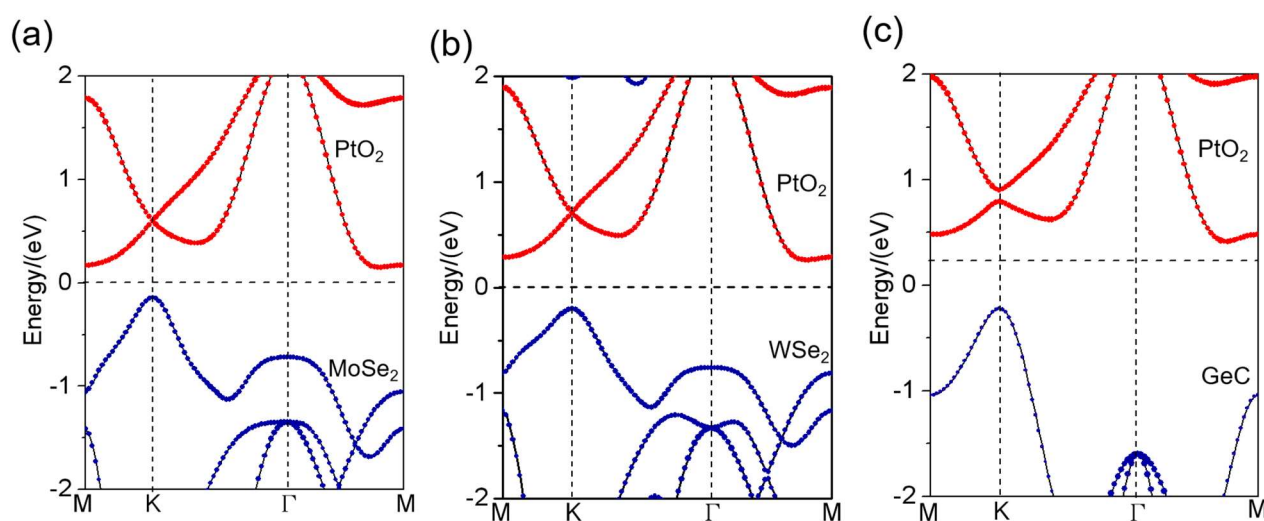


**Fig. S6** Projected band structure at HSE06 level of the heterojunction (a) PtO<sub>2</sub>/MoSe<sub>2</sub>, (b) PtO<sub>2</sub>/WSe<sub>2</sub> and (c) PtO<sub>2</sub>/GeC, where Fermi level is set to zero level and indicated by the horizontal black dashed line.

Similar to the heterojunction PtO<sub>2</sub>/MoSe<sub>2</sub>, it can be seen that most of CBM is from PtO<sub>2</sub>, while WSe<sub>2</sub> (GeC) contributes to the VBM in heterojunction PtO<sub>2</sub>/WSe<sub>2</sub> (GeC), leading to the direct Z-scheme systems. Then, the reduction reaction occurs on WSe<sub>2</sub> (GeC), while oxidation reaction is on PtO<sub>2</sub>.



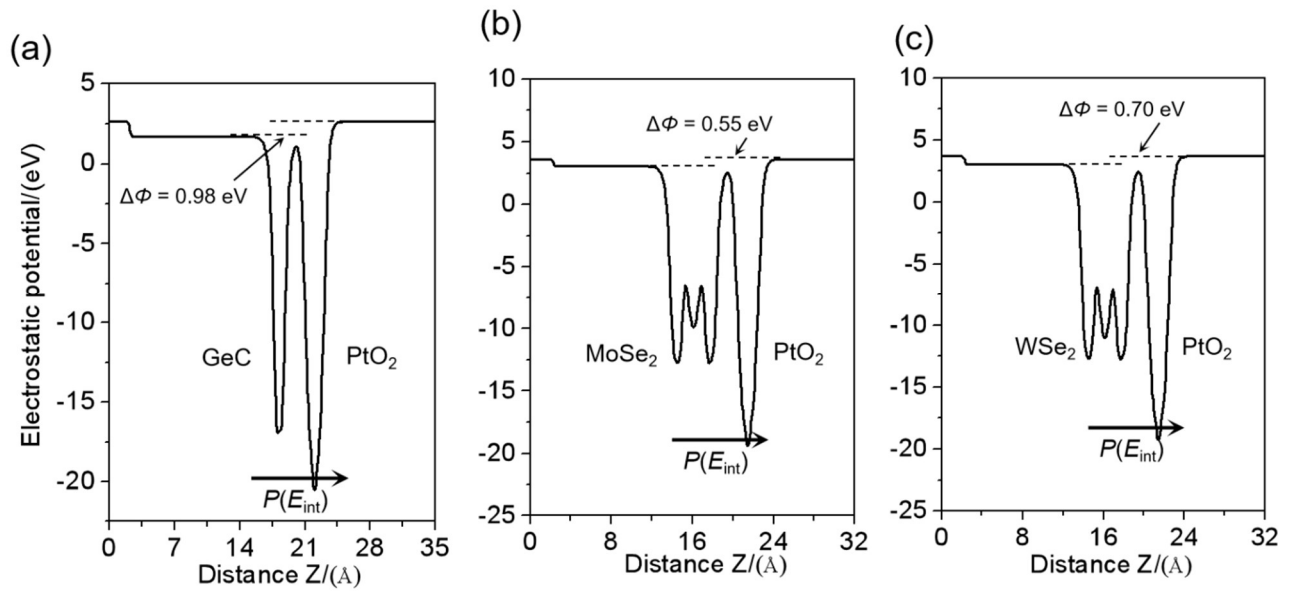


**Fig. S7** Electrostatic potential of the heterojunction (a) PtO<sub>2</sub>/GeC, (b) PtO<sub>2</sub>/MoSe<sub>2</sub>, and (c) PtO<sub>2</sub>/WSe<sub>2</sub>. The arrows represent the direction of polarization ( $P$ ) and internal electric field ( $E_{int}$ ).

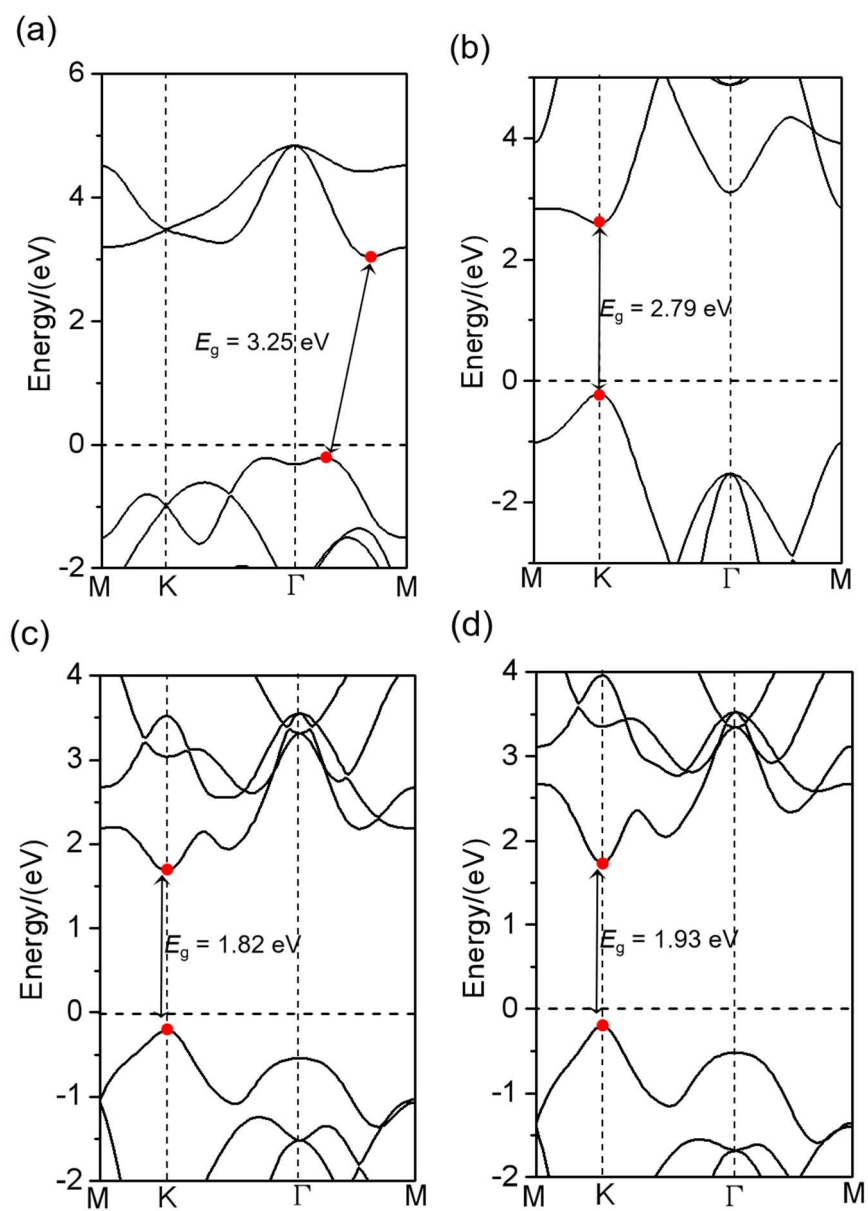


**Fig. S8** Electronic band structure at HSE06 level of the isolated monolayers (a) PtO<sub>2</sub>, (b) GeC, (c) MoSe<sub>2</sub>, and (d) WSe<sub>2</sub>, where Fermi level is set to zero level and indicated by the horizontal black dashed line. The red dots represent the CBM and VBM.

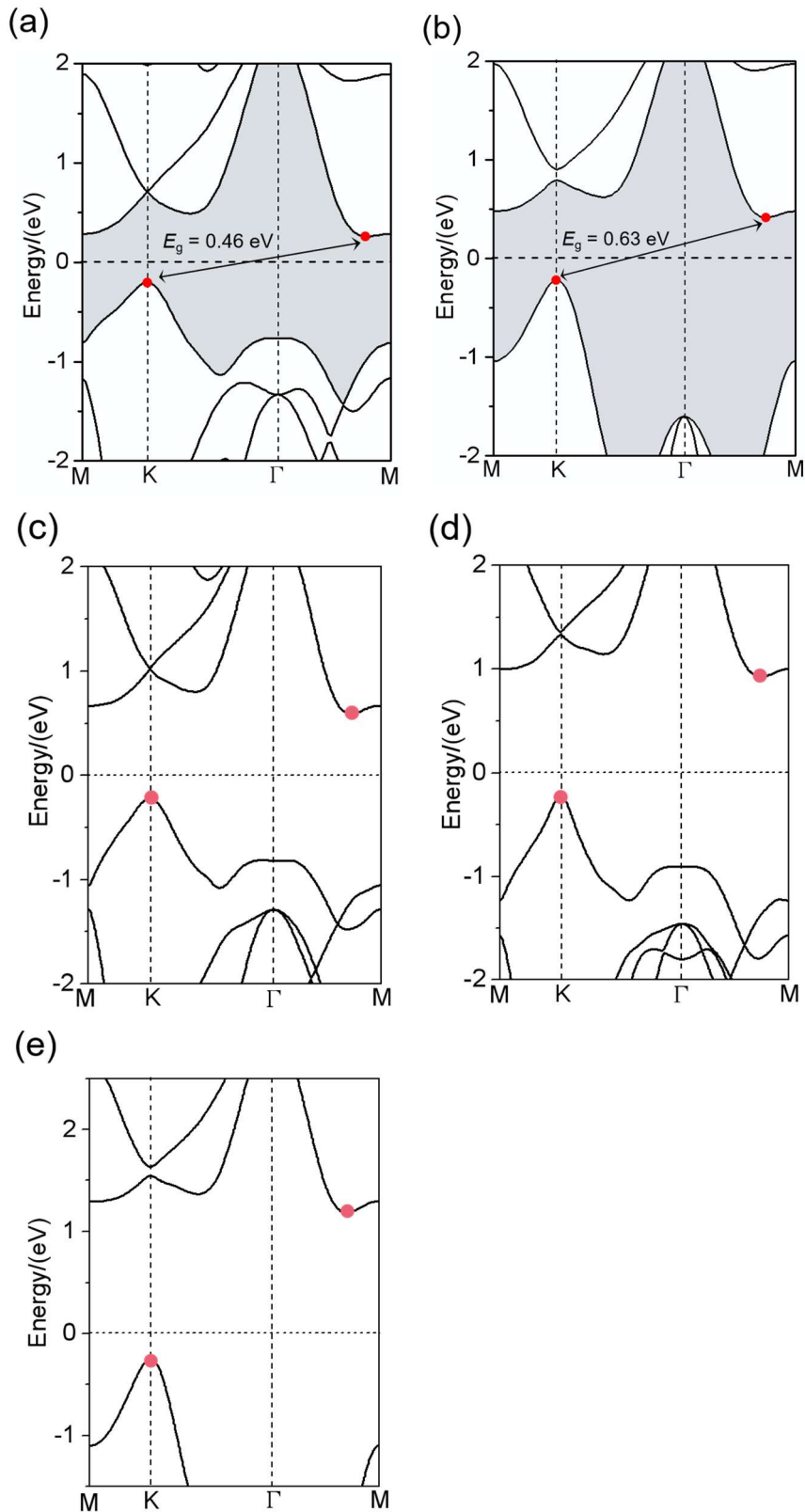


**Fig. S9** HSE06 band structure of the heterojunction (a) PtO<sub>2</sub>/WSe<sub>2</sub>, and (b) PtO<sub>2</sub>/GeC.  $G_0W_0$  band structure of the heterojunction (c) PtO<sub>2</sub>/MoSe<sub>2</sub>, (d) PtO<sub>2</sub>/WSe<sub>2</sub> and (e) PtO<sub>2</sub>/GeC, where Fermi level is set to zero level and indicated by the horizontal black dashed line. The red dots represent the CBM and VBM.

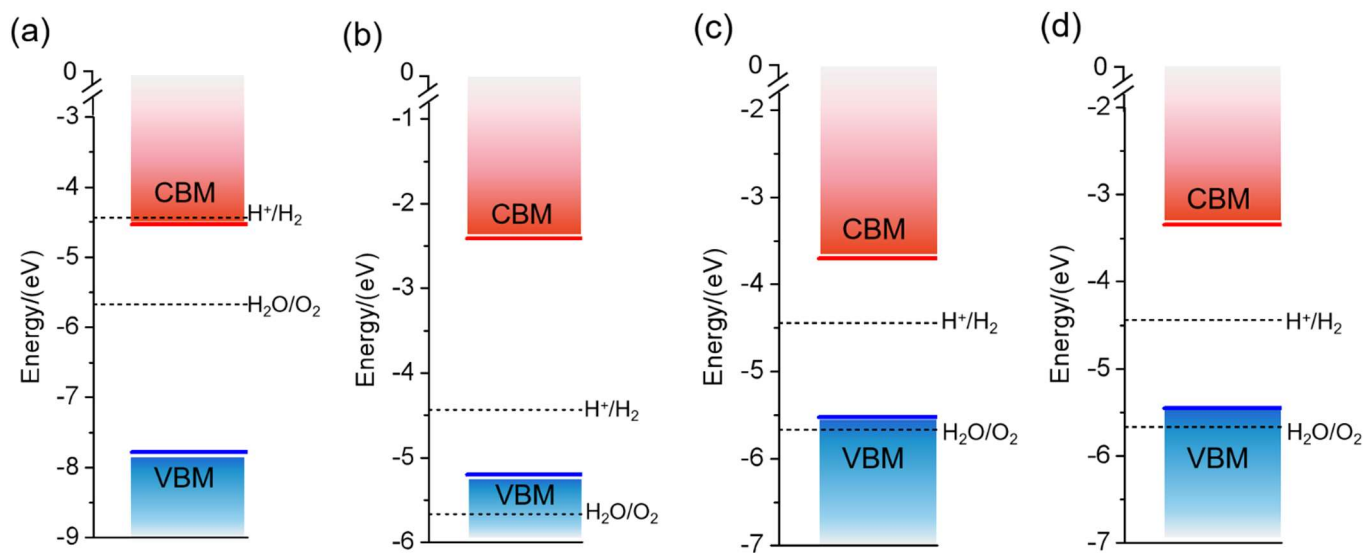


**Fig. S10** Band alignments of the monolayers (a) PtO<sub>2</sub>, (b) GeC, (c) MoSe<sub>2</sub>, and (d) WSe<sub>2</sub>, where the black dashed lines represent the reduction potential and oxidation potential of water splitting.

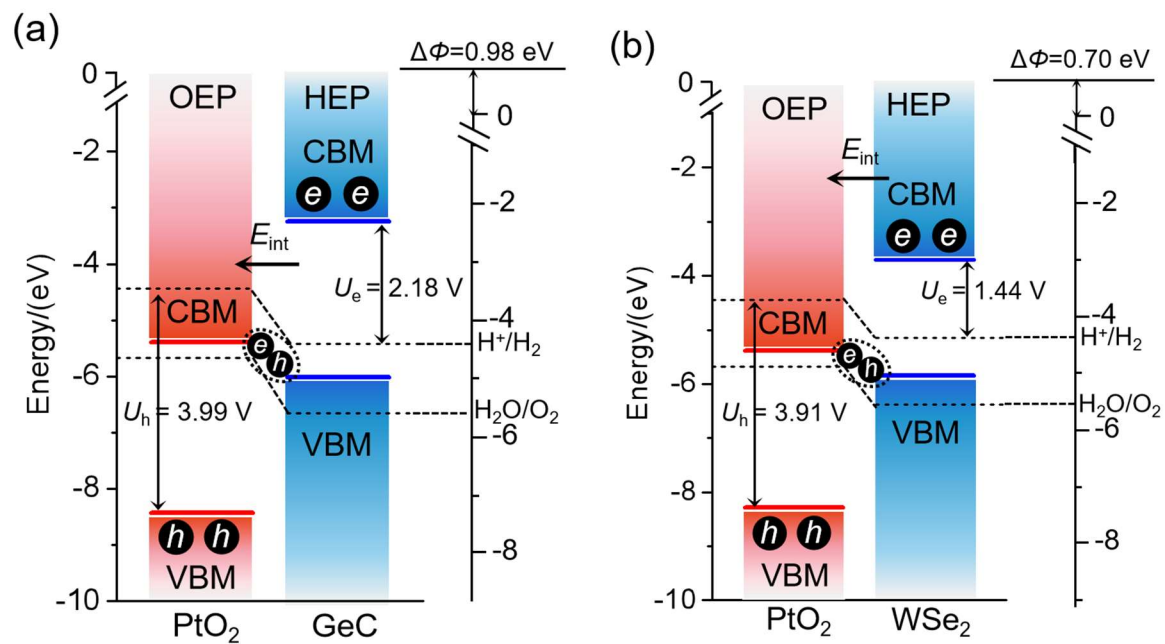


**Fig. S11** Band alignments of the heterojunction (a) PtO<sub>2</sub>/GeC, and (b) PtO<sub>2</sub>/WSe<sub>2</sub>. The horizontal black dashed lines represent the reduction potential and oxidation potential of water splitting, and the potentials of HEP side are bended downward by  $\Delta\Phi$ .

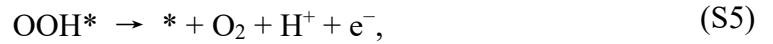
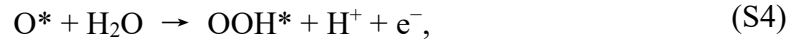
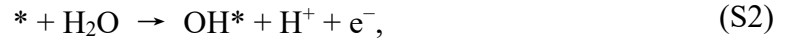
## 1. Gibbs free energies

The Gibbs free energy difference ( $\Delta G$ ) from one step to next step involved in the photocatalytic redox reactions can be evaluated using the method proposed by Norskovet et.al. [1] At pH = 0, the formula without the light irradiation can be defined as below:

$$\Delta G = \Delta E + \Delta E_{ZPE} - T\Delta S, \quad (S1)$$

where  $\Delta E$  is the adsorption energy,  $\Delta E_{ZPE}$  and  $\Delta S$  are the difference in zero point energy and entropy difference between the adsorbed state and the gas phase, respectively.

The half OER is considered herein, which are presented step by step as follows:



For the half HER, it can be described in the following steps:



where \* represents the substrate materials for the adsorptions, and O\*, OH\*, OOH\* and H\* represent the adsorbed intermediates during the redox reaction.

The Gibbs free energy difference of each step included in the half OER and HER is available based on the following expressions, in which the impact of extra potential and pH is taken into account:

$$\Delta G_1 = G_{OH^*} + \frac{1}{2}G_{H_2} - G_{H_2O} - G_* + \Delta G_U - \Delta G_{pH}, \quad (S8)$$

$$\Delta G_2 = G_{O^*} + \frac{1}{2}G_{H_2} - G_{OH^*} + \Delta G_U - \Delta G_{pH}, \quad (S9)$$

$$\Delta G_3 = G_{OOH^*} + \frac{1}{2}G_{H_2} - G_{O^*} - G_{H_2O} + \Delta G_U - \Delta G_{pH}, \quad (S10)$$

$$\Delta G_4 = G_* + G_{O_2} + \frac{1}{2}G_{H_2} - G_{OOH^*} + \Delta G_U - \Delta G_{pH}, \quad (S11)$$

$$\Delta G_5 = G_{H^*} - G_* - \frac{1}{2}G_{H_2} + \Delta G_U + \Delta G_{pH}, \quad (S12)$$

$$\Delta G_6 = G_* + \frac{1}{2}G_{H_2} - G_{H^*} + \Delta G_U + \Delta G_{pH}, \quad (S13)$$

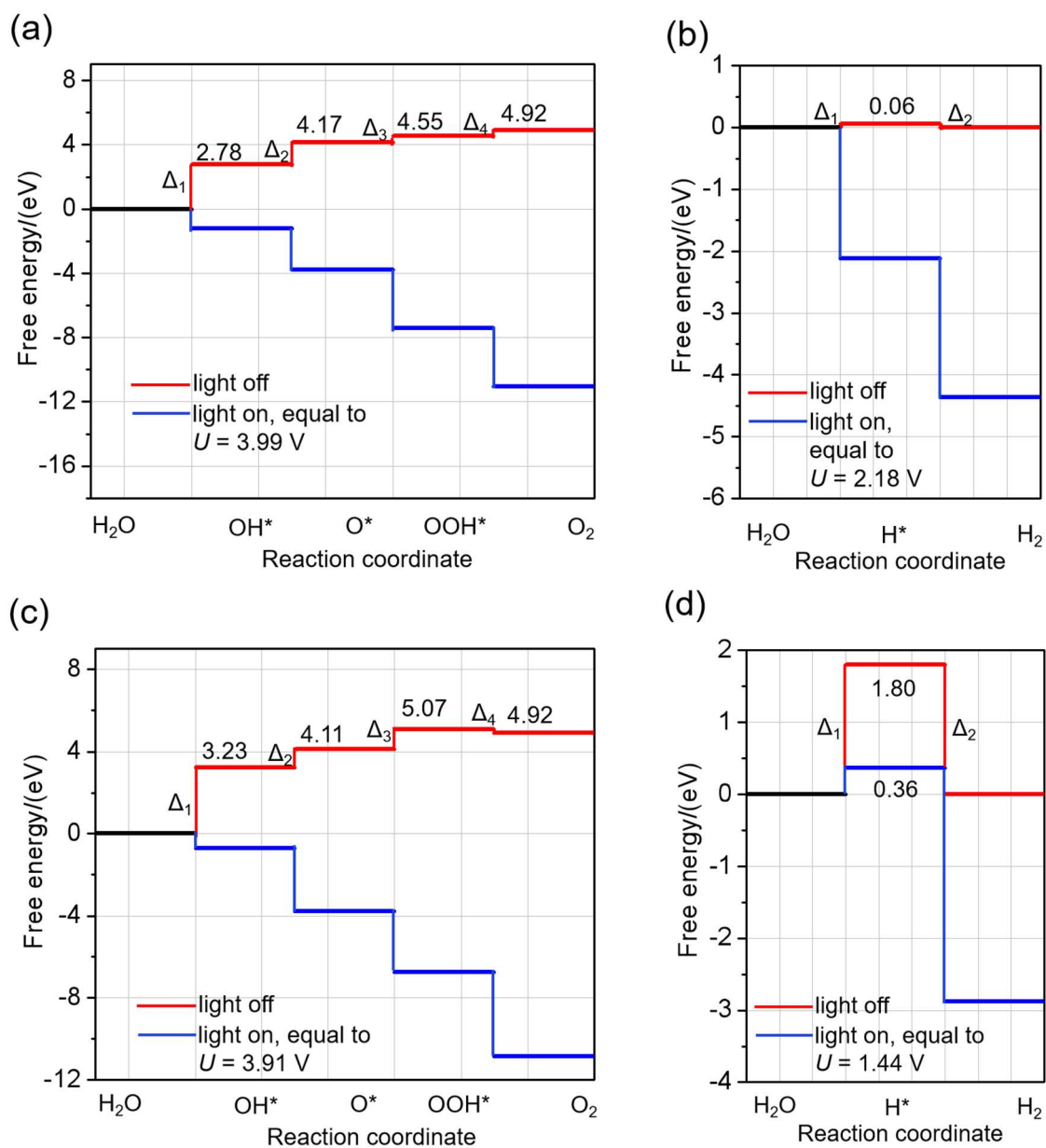


**Fig. S12** Gibbs free energy profiles of OER and HER on the heterojunction (a-b) PtO<sub>2</sub>/GeC, and (c-d) PtO<sub>2</sub>/WSe<sub>2</sub> at pH = 0.

## References

- [1] J. K. Nørskov, J. Rossmeisl, A. Logadottir and L. Lindqvist, *J. Phys. Chem. B*, 2004, **108**, 17886–17892.